journal

J. Am. Ceram. Soc., 78 [3] 529–38 (1995)

Group II Tris(glycolato)silicates as Precursors to Silicate Glasses and Ceramics

Pallavi Kansal* and Richard M. Laine*

Department of Materials Science and Engineering, University of Michigan, Ann Arbor, Michigan 48109-2136

Group II tris(glycolato)silicates, $MSi(OCH_2CH_2O)_3$ (where M = Ba, Ca, Mg), can be synthesized directly by reaction of silica with ethylene glycol and alkaline-earth (group II) oxides at 200°C. These hexa-alkoxy silicates serve as precursors to silicate glass and ceramic powders. They are readily modified by exchange with longer-chain diols into processable polymer precursors. These rheologically useful precursors may provide access to silicate or aluminosilicate powders, thin films, fibers, and coatings. Thus, we have examined the utility of hexacoordinate glycolatosilicates as model precursors. Pyrolysis of the compounds, $MSi(OCH_2CH_2O)_3$, in air transforms them to their anticipated ceramic products, $MO{\cdot}SiO_2$. The phase transformations and chemical changes that occur during pyrolysis were characterized using X-ray powder diffractometry (XRD), diffuse reflectance infrared Fourier transform spectroscopy (DRIFTS), thermal gravimetric analysis (TGA), differential thermal analysis (DTA), and scanning electron microscopy (SEM). The hexacoordinate glycolatosilicates oxidatively decompose at ≈300°C to form amorphous materials. Moderate to significant quantities of the group II carbonates, MCO_3 (15–50 wt%), form coincidentally as the amorphous intermediates trap CO_2 generated by ligand oxidation. At ≈900°C, the amorphous materials crystallize into the expected, phase-pure, $MO{\cdot}SiO_2$.

I. Introduction

WE HAVE recently demonstrated that it is possible to synthesize group I pentacoordinate anionic glycolatosilicate complexes by direct reaction of group I hydroxides with fused silica, silica gel, or even beach sand in the presence of excess ethylene glycol (EG) in good yields, with high purities:[1–4]

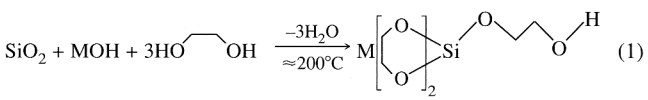

(1)

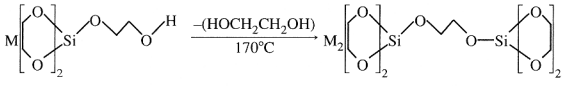

(2)

M = Li, Na, K, Cs

In related work, we found that group II metal (Ba, Ca, or Mg) oxides react with SiO_2 and EG to form hexacoordinate, dianionic, tris(glycolato)silicate complexes (see Experimental Section) as shown below:[5]

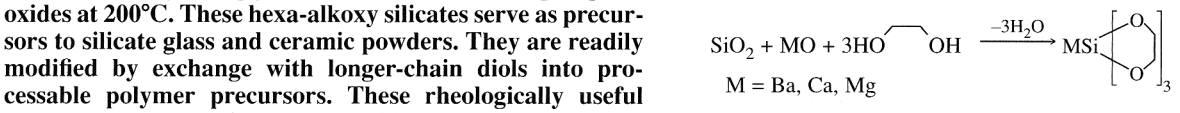

(3)

M = Ba, Ca, Mg

When MgO is used in reaction (3), the yields are so poor that we developed an alternate synthesis (see Experimental Section) as shown in reactions (4) and (5):

$$Mg + 2MeOH \rightarrow Mg(OMe)_2 \quad (4)$$

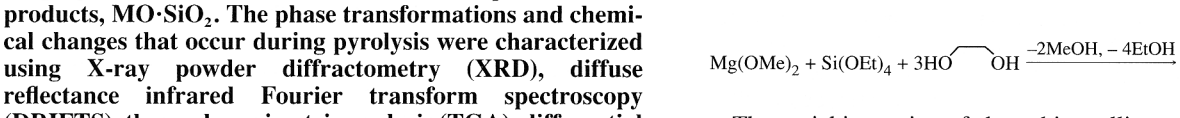

(5)

The stoichiometries of these bimetallic complexes suggest that they might be of use as precursors to simple group I and II silicate glass and ceramic powders, and eventually in the formulation of aluminosilicate glass and ceramic powder precursors. In addition, because the EG ligands in these crystalline complexes readily exchange with longer-chain diols to form rheologically useful polymeric derivatives, these complexes have potential for fabricating thin silicate (and aluminosilicate) films, membranes, coatings, or fibers. Furthermore, because of the low temperatures, simple one (or two) step syntheses, and the inexpensive raw materials, in principle, the processing methods described here could considerably reduce processing costs for silicates and aluminosilicates compared to the conventional, high-temperature melt processing methods currently in use. Hence, this general approach to silicate and aluminosilicate glasses and ceramics appears to offer considerable promise for the future.

The first step in these studies was to model the pyrolytic transformations of the group I pentacoordinate polymeric silicates, using the glycolatosilicates as models.[6] The pentacoordinate silicon complexes $MSi(OCH_2CH_2O)_2OCH_2CH_2OH$, synthesized via reaction (1), were found to dimerize on heating (170°C) *in vacuo*, to form $M_2Si_2(OCH_2CH_2O)_5$, reaction (2). On pyrolysis, the dimers typically transform to the anticipated ceramic products, $M_2O{\cdot}2SiO_2$, at 500–700°C, with primary weight loss (i.e., oxidative removal of EG ligands) occurring at 335–395°C. During oxidative decomposition, small amounts of metal carbonates form coincidentally, as the oxidation product, CO_2, reacts with the amorphous intermediates that form initially. Further heating to 900°C eliminates any residual carbonates and provides nearly phase-pure, crystalline materials, as determined by XRD, FTIR, SEM, TGA, DTA, and chemical analyses.[6]

The second step in these studies is an examination of the pyrolytic behavior of the group II, hexacoordinate tris(glycolato)silicates, as models of polymeric derivatives and as a prelude to detailed work on celsian ($BaO{\cdot}Al_2O_3{\cdot}2SiO_2$)[4] and cordierite ($2MgO{\cdot}2Al_2O_3{\cdot}5SiO_2$)[7] aluminosilicate precursors. It is worth noting that the silicate products, especially $CaO{\cdot}SiO_2$, provide good-to-excellent, lightweight refractory materials.[8]

C. J. Brinker—contributing editor

Manuscript No. 193536. Received June 1, 1994; approved October 17, 1994.
Supported by the U.S. Army Research Laboratory and Army Research Office through Contract No. DOD-C-DAAL04-91-C-0068 and ASSERT Grant No. DOD-G-DAAL03-92-G-0053, and by the Office of Naval Research through Grant No. N00014-92-J-1711.
*Member, American Ceramic Society.

In the following, we present studies on the pyrolytic behavior (in air) of tris(glycolato)silicates, $MSi(OCH_2CH_2O)_3$, where M = Ba, Ca, or Mg, synthesized via reactions (3) to (5). These studies delineate the effects of temperature and time on the decomposition and crystallization processes, whereby $MSi(OCH_2CH_2O)_3$ transforms into phase-pure, crystalline $MO{\cdot}SiO_2$. Our objectives are to delineate the processing parameters whereby the hexacoordinate glycolatosilicates can be most easily converted into ceramic powders, and the related polymers into thin films, fibers, coatings, and membranes.

II. Experimental Section

(1) Syntheses

The general procedures for handling air- and moisture-sensitive glycolatosilicates, as well as solvent preparation, are described in the previous paper.[6] All of the reactions were run under N_2 with careful exclusion of moisture. The analytical data for the isolated compounds are recorded in Table I.

(A) $BaSi(OCH_2CH_2O)_3{\cdot}3HOCH_2CH_2OH$: Barium glycolatosilicate is prepared in a manner similar to the calcium complex (see below). Its complete synthesis and characterization by single-crystal diffraction studies are reported elsewhere.[5]

(B) $CaSi(OCH_2CH_2O)_3{\cdot}3HOCH_2CH_2OH$: Calcium oxide (28.04 g, 0.5 mol), SiO_2 (30.04 g, 0.5 mol), and excess EG (500 mL) were mixed in a 1-L schlenk flask. The mixture was heated to distill off EG and byproduct water, at ≈200°C, under N_2, with constant mechanical stirring (reaction (3)). The silica and alkaline-earth oxide dissolve readily with continuous distillative removal of EG and water. The reaction goes clear in 1–2 h after 350–400 mL of EG distills off. As the distillation continues, the clear solution becomes viscous and the product starts to precipitate out. The reaction is allowed to cool. A large solid mass forms overnight. This mass is filtered through a medium frit and washed with 300 mL of distilled acetonitrile to remove residual EG. A fine white powder is obtained on vacuum drying the precipitate at ≈70°C. The corresponding chemical analyses discussed below indicate that this comound is also hexacoordinated. Furthermore, the ^{29}Si and ^{13}C solid-state NMR, which will be presented elsewhere, support this assignment.

(C) $MgSi(OCH_2CH_2O)_3{\cdot}2.25HOCH_2CH_2OH$: Generally, the alkaline-earth glycolatosilicates are synthesized directly from SiO_2 and metal oxide dissolved in EG. However, MgO is not very soluble in EG, and the reaction with SiO_2, besides being extremely slow (reaction (3)), results in low yields. Therefore, the compound is prepared by reaction of $Mg(OCH_3)_2$ (reaction (4)) with tetraethoxysilane, $Si(OC_2H_5)_4$, in the presence of excess EG (reaction (5)).

Mg metal (12.15 g, 0.5 mol) and excess MeOH (200 mL), with a catalytic amount of $HgCl_2$, are placed in a 1-L schlenk flask. The reaction flask is cooled because the reaction is highly exothermic. After 15–20 min, almost all of the Mg metal dissolves. A small amount of black residue is removed by filtering through celite to give a clear, light yellow solution. Tetraethoxysilane (104.2 g, 0.5 mol) and EG (169 mL, 3 mol) are added to this solution and the solution is heated and refluxed continuously for 1–2 h. The MeOH, EtOH, and EG are distilled off. As distillation continues, the solution becomes increasingly viscous and cloudy. The reaction is then stopped and filtered through a medium frit to give a clear, light yellow solution (some of the reaction product polymerizes and is left in the frit). A fine white powder is obtained on vacuum removal of solvent at 70°C. The corresponding chemical analyses presented below indicate that this compound is also hexacoordinated. Additionally, the ^{29}Si and ^{13}C solid-state NMR, which will be presented elsewhere, support this assignment.

(2) Precursor Sample Treatment

All of the isolated compounds are readily recrystallized by redissolution in a minimum volume of hot EG. On cooling, the crystalline compounds are filtered off, washed with acetonitrile, and vacuum dried at 70°C, to remove any residual acetonitrile, but retain EG molecules of recrystallization (see Results and Discussion). These compounds were then characterized by TGA and chemical analysis. The TGA ceramic yields were used to calculate the number of EG molecules of recrystallization per silicon center and calculate theoretical H and C contents. Chemical analyses confirmed, with a high degree of accuracy, the calculated ceramic yields. Thus, the precursor powders were easily purified. The precursory powders were also analyzed by XRD to confirm their crystalline nature.

All of the hexacoordinate glycolatosilicates synthesized above were then vacuum dried at 170°C (4–5 h), to free the $MSi(OCH_2CH_2O)_3$ precursors of most EG solvate as determined by TGA (see Results and Discussion) ceramic yields. The 170°C-dried compounds were used as samples for the pyrolysis studies. These products are moisture sensitive and also react readily with CO_2; therefore, they were stored in an inert atmosphere of a Vacuum Atmospheres Model No. MO40-2-Dri-Lab glove box (Vacuum Atmospheres Co., Hawthorne, CA).

(3) Pyrolyses

The procedures used are similar to those described for the pyrolysis studies of the pentacoordinate glycolatosilicates.[6] Samples of the individual precursors were pyrolyzed in a single-zone, Lindberg tube furnace (Model No. 58114, Watertown, WI), equipped with a Eurotherm programmable temperature controller (Model No. 818P, Northing, England). Samples (1–2 g) were packed in an alumina boat and placed inside a ported quartz tube, inside the glove box. The quartz tube was then sealed with a cap, taken out of the glove box, inserted into the furnace, and connected to a supply of dry, compressed air. The individual samples were heated at 10°C/min in flowing (synthetic) air to selected temperatures (300°, 500°, 700°, 900°, and 1000°C) and held there for 2 h. The pyrolyzed samples were unloaded inside the glove box and stored there. The pyrolyzed samples were not exposed to ambient atmosphere during the transfer process.

Note: The dry, compressed air was free of any H_2O or CO_2.

(4) Characterization

The phase transformations and chemical changes that occur during pyrolytic transformation of the precursors to amorphous and/or crystalline materials were characterized using powder X-ray diffractometry (XRD), diffuse reflectance infrared Fourier transform spectroscopy (DRIFTS), scanning electron microscopy (SEM), thermal gravimetric analysis (TGA), and

Table I. Chemical Analyses for Group II Tris(glycolato)silicates

Compound†	MW	Ceram yield (wt%)	Sample	C (wt%)	H (wt%)
$BaSi(OCH_2CH_2O)_3{\cdot}3(\ )$	524.70	39.5	Calcd	27.41	5.70
			Exptl	26.90	5.66
$CaSi(OCH_2CH_2O)_3{\cdot}3(\ )$	429.63	27.0	Calcd	33.15	6.91
			Exptl	32.53	6.70
$MgSi(OCH_2CH_2O)_3{\cdot}2.25(\ )$	370.37	27.1	Calcd	33.89	6.85
			Exptl	33.98	7.19

†( ) refers to ethylene glycol, $HOCH_2CH_2OH$.

differential thermal analysis (DTA). Chemical analyses were performed in the Department of Chemistry, University of Michigan, Ann Arbor, MI. All of the data for the following studies are presented in the Results and Discussion section.

(A) XRD: The XRD patterns were determined using a Rigaku rotating anode goniometer (Rigaku Denki Co. Ltd., Tokyo, Japan). Powder samples (100–200 mg) were ground with an alumina mortar and pestle, packed in a glass specimen holder, and placed in the goniometer. Scans were continuous from 5° to 80° 2θ at a scan rate of 10° 2θ/min using 0.05° 2θ increments and Cu$K\alpha$ (λ = 1.542 Å) radiation. The peak positions and the relative intensities of the powder patterns were identified by comparing with standard JCPDS files.

(B) DRIFTS: The DRIFT spectra were recorded on a Mattson Galaxy Series FTIR 3000 spectrometer (Mattson Instruments, Inc., Madison, WI). Optical-grade, random cuttings of KBr (International Crystal Laboratories, Garfield, NJ) were ground using an alumina mortar and pestle and transferred to a schlenk flask. The KBr powder was vacuum dried for 0.5 h and then taken inside the glove box. DRIFT samples were prepared in the glove box by mixing 0.3–1.0 wt% of the sample to be analyzed with the vacuum-dried KBr.

Sample concentrations were kept below 1 wt% to ensure adherence to Beer's law. The dilute samples prepared in KBr were subsequently packed firmly in the sample holder, leveled off at the upper edge to provide a smooth surface, and transferred to the FTIR sample chamber (brief exposure to air), which was flushed constantly with N_2. A minimum of 64 scans were collected for each sample at a resolution of ± 4 cm^{-1}. Peak positions were identified using a standard peak searching program.

(C) Thermal Analytical Techniques: TGA and DTA of the hexacoordinate silicates were performed on a 2950 thermal analysis instrument and a 2910 differential scanning calorimeter (TA Instruments, Inc., New Castle, DE), respectively. TGA samples averaging 10–15 mg were loaded on a platinum pan and heated in flowing (60 cm^3/min) dry air, at 10°C/min to 1000°C. DTA measurements (≈20 mg samples) were performed using platinum crucibles, under a continuous flow (50 cm^3/min) of dry air, at 10°C/min to 1200°C. Calcined Al_2O_3 (Aluminum Co. of America, Pittsburgh, PA) was used as a reference.

(D) Scanning Electron Microscopy: Powder morphologies were examined using a Hitachi S-800 scanning electron microscope (Hitachi Tokyo, Japan) operating at 5 keV. SEM samples were prepared by mounting pyrolyzed powder samples on an aluminum stub using a double-stick tape. Samples were sputter coated with a layer of Au/Pd for 45 s at 10 mV, to enhance their conductivity.

III. Results and Discussion

With the exception of the Mg compound, the MSi-$(OCH_2CH_2)_3$ complexes were easily prepared directly from silica and the metal oxide. Stoichiometrically correct mixtures of the oxides in dry EG, used as both solvent and reactant, were heated to distill off EG (≈200°C) and coincidentally drive off water that forms as reaction (3) proceeds. On heating for 1–2 h, the solids dissolved and the reaction volume was reduced until a viscous liquid resulted. On cooling, the products crystallized out in essentially quantitative yield. In the case of the Mg compound, $Mg(OMe)_2$ was first formed in MeOH, reaction (4), and an equivalent amount of $Si(OEt)_4$ and ≈3 equiv of EG were then added. The resulting solution was heated to reflux, reaction (5), for a few hours, reduced in volume, cooled, and filtered to give a clear solution which on vacuum drying (70°C) gives the expected product.

The products from all of the reactions were easily recrystallized by redissolving (with heat) in a minimum volume of EG. On cooling, the products crystallized out as solvates containing excess amounts (2–3 mol) of EG of recrystallization. As described in detail in the following sections, these products were first characterized by chemical and thermal analyses, which provided information about precursor purity and degree of solvation. The characterized complexes, $MSi(OCH_2CH_2O)_3 \cdot$ 2–3EG, were then dried at 170°C *in vacuo* prior to conducting pyrolytic decomposition studies.

TGA profiles of the dried samples, in dry air, were then obtained to establish a preliminary understanding of mass loss events as a function of pyrolysis temperature. Coincident DTA studies were conducted to further elucidate the mass loss events observed in the TGA. Generally, TGAs of all three glycolates show major mass losses at 170–400°C (20–40%), due to oxidative decomposition of the glycolato ligands, as corroborated by exotherms seen in DTAs. The thermal analysis data provide temperature windows that define optimum bulk pyrolysis temperatures. For example, most of the precursors decompose just above 300°C; therefore, the first stage in the bulk pyrolysis studies examined the effects of a 2-h hold at 300°C, on dried precursor. The object was to hold the sample for a sufficient period of time to ensure complete decomposition of the glycolate ligands but limit diffusion that might lead to phase transformations. Furthermore, most of the materials crystallize by 900°C, so pyrolysis temperatures of 500° and 700°C were chosen to look for the onset of crystallization and/or characterize the amorphous materials at higher temperatures (XRD and DRIFTS).

Generally, the pyrolyzed samples first transform into amorphous materials that contain some carbonate (CO_3^{2-}) and bicarbonate (HCO_3^-) species (identified by DRIFTS). The amount of carbonate species was calculated from the TGA mass loss events. These events were corroborated by endotherms, around the same temperature, in the DTA. On continued heating, the amorphous carbonate-containing materials crystallized into the line compounds $MO \cdot SiO_2$, as expected based on the initial $MSi(OCH_2CH_2O)_3$ composition. The associated crystallization processes were followed by XRD, whereas DRIFT spectroscopy proved useful in identifying atomic-level materials reorganization processes. The chemical analyses and decomposition patterns of all three precursors are discussed below, individually.

(1) $BaSi(OCH_2CH_2O)_3$

(A) Thermal Analysis: The reported crystal structure for barium glycolatosilicate indicates that each unit cell contains 3.25 EG molecules of recrystallization per silicon center.[5] A TGA of 70°C-dried $BaSi(OCH_2CH_2O)_3 \cdot 3HOCH_2CH_2OH$ (see Experimental Section) powder produced for the current studies, gave a ceramic yield of 39.5%. Assuming the end product is $BaO \cdot SiO_2$ at 1000°C, the number of EG molecules of recrystallization per silicon center can be calculated. Based on the 39.5% ceramic yield, the precursor appears to have 3.00 EG molecules of recrystallization. This value is confirmed by the chemical analyses recorded in Table I. The calculated C content with 3.00 EGs is 27.41 wt%, which is within experimental error of the experimental value of 26.90. Likewise, the calculated H content is 5.70 wt% vs an experimental value of 5.66. This good correlation indicates the high purity with which these novel complexes are easily synthesized.

The crystalline nature of this solvate complex, aside from the previously published single-crystal structure, is further evidenced by its XRD powder pattern (see below). If the 70°C-dried precursor powder is further heated at 170°C (4–5 h) under vacuum, the EG molecules of solvation volatilize. The recovered material no longer exhibits a distinct XRD powder pattern. Thus, heating to remove EG solvate molecules produces an amorphous precursor powder, which in principle should still conform to the $BaSi(OCH_2CH_2O)_3$ formula, as suggested by the TGA shown in Fig. 1.

The Fig. 1 TGA of the 170°C-treated $BaSi(OCH_2CH_2O)_3$ shows a ceramic yield of 59.9%, which is ≈2% lower than the calculated value of 61.8% (Table II). This small difference is likely due to some fractional retention of EGs of crystallization, even following 4–5 h heating at 170°C. As in the group I

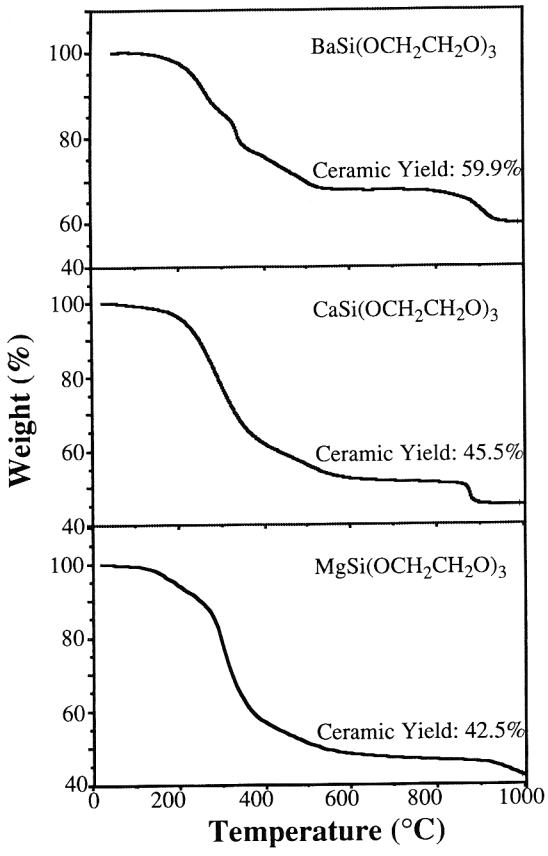

Fig. 1. TGA profile of $MSi(OCH_2CH_2O)_3$. Ramp was 10°C/min in synthetic air.

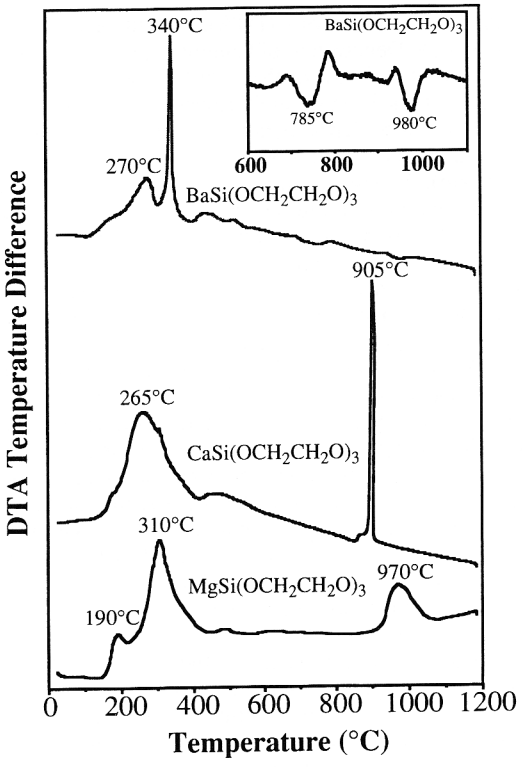

Fig. 2. DTA profile of $MSi(OCH_2CH_2O)_3$. Ramp was 10°C/min in synthetic air.

glycolatosilicates, the initial mass loss occurs in the range 200–370°C and is due to oxidative decomposition of the glycolate ligands. A further mass loss (≈7.5 wt%, based on initial precursor mass) is observed at 850–980°C and results from the decomposition of $BaCO_3$ ($T_d \approx 980$°C) coincident with crystallization of $BaO{\cdot}SiO_2$. If we assume that this mass loss is solely due to evolution of CO_2, we can back calculate the mass of $BaCO_3$ present at ≈850°C. This calculation indicates that at 850°C, almost 50.0 wt% of the total material is $BaCO_3$. If we assume that the final product is phase-pure $BaO{\cdot}SiO_2$, then we can suggest an apparent distribution of compounds at 850°C with the approximate ratios $BaO:1.5BaCO_3:2.5SiO_2$.

The corresponding DTA of $BaSi(OCH_2CH_2O)_3$ (Fig. 2) shows exotherms at 270° and 340°C resulting from oxidation of the glycolatosilicate ligands to form amorphous $BaO{\cdot}SiO_2$ (see XRD). The exotherm at 270°C, which is not seen in the corresponding group I studies, most probably results from oxidation of the remaining fraction of EG solvate molecules (see below).

Table II. Calculated and Experimental Ceramic Yields for the $MSi(OCH_2CH_2O)_3$, Where M = Ba, Ca, Mg

$MSi(OCH_2CH_2O)_3$	Yield (%)† Calcd	Exptl
Barium	61.8	59.9
Calcium	46.8	45.5
Magnesium	43.2	42.5

†The calculated yields are based on assuming $MO{\cdot}SiO_2$ is the end product. The experimental values are the TGA yields at 1000°C.

The TGA shows mass loss in this region, although no distinct event is observed.

The DTA does not show any defined endotherm corresponding to carbonate decomposition (mass loss in the TGA) or an exotherm due to crystallization (see XRD below), despite the fact that the DTAs of the calcium and magnesium glycolatosilicates show distinct exotherms for crystallization. One possible explanation is that the expected endotherm arising from thermally promoted decomposition of $BaCO_3$ exactly balances the anticipated exotherm resulting from crystallization of $BaO{\cdot}SiO_2$ (see XRD below). However, this seems unlikely in view of the fact that no endotherms are seen for decomposition of the calcium or magnesium carbonates. Figure 3 shows the DTA for an authentic sample of $BaCO_3$. The 820°C endotherm corresponds to γ-to-β phase transformation. The second endotherm at 980°C corresponds to decomposition to BaO.

To further understand the absence of DTA peaks corresponding to CO_2 mass loss and crystallization events, a somewhat different study was performed. It was assumed that the sample size used for the complete DTA experiment might not produce

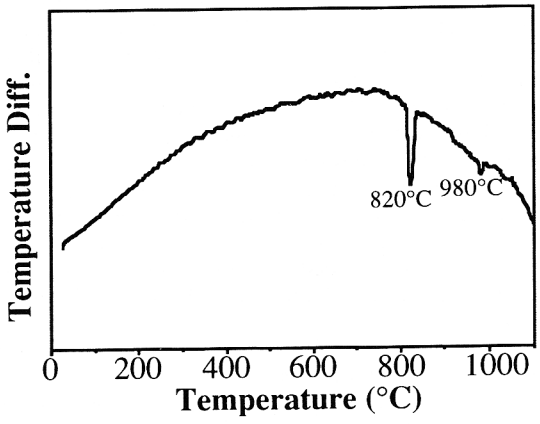

Fig. 3. DTA of $BaCO_3$. Ramp was 10°C/min in synthetic air.

sufficient material on heating above 350°C, to permit good resolution of the thermal events occurring at higher temperatures. Thus, a 170°C sample was heated to 500°C for 2 h, to fully oxidize off the EG ligands, without heating to temperatures that would favor diffusion and crystallization. The amorphous 500°C sample was then heated in the DTA at 5°C/min to 1200°C (see inset, Fig. 2). The inset appears to show two small endotherms and two or three exotherms.

We suggest that the first endotherm (see inset) at 785°C corresponds to the barium carbonate γ-to-β phase transformation. The reason for the 40°C difference in transformation temperatures is likely due to the composite nature of the material, wherein the smaller $BaCO_3$ particles (compared to the bulk material in Fig. 3) have higher surface energies that drive the phase transformation. The second endotherm at 980°C corresponds to decomposition of $BaCO_3$ that has not yet reacted with SiO_2 to form $BaO{\cdot}SiO_2$. This can be interpreted to indicate that the microstructure of the segregated phases is not uniform, as supported by the relatively broad weight loss (850–980°C) associated with carbonate decomposition.

If there are significant variations in microstructure, then the exotherms at 780–800° and 940–950°C might both correspond to $BaO{\cdot}SiO_2$ crystallization resulting from decomposition of different-sized $BaCO_3$ particles followed by reaction with free SiO_2. However, a more realistic interpretation is that the 780–800°C exotherm is due to the direct reaction of free BaO with SiO_2. The 940–950°C exotherm then corresponds to a process that begins with decomposition of $BaCO_3$ to CO_2 and BaO, followed by reaction of this BaO with remaining SiO_2. The combination of processes, leading to crystallization of $BaO{\cdot}SiO_2$, occurs over a large temperature range and thus explains the absence of a large crystallization exotherm, as seen for the other two compounds; see below. Finally, the peak at 680–700°C may or may not correspond to an exotherm; we suspect that it corresponds to a rise in the DTA baseline. An alternate explanation is that it is part of a broad exotherm at 690–800°C that is interrupted by the γ-to-β endotherm. The relatively low temperature would result in low diffusion rates, hence a broad exotherm.

(B) XRD: The XRD patterns displayed in Fig. 4 show the phase development upon pyrolysis at selected temperatures following a 2-h hold. Figure 4 also shows the powder pattern of the 70°C-dried Ba precursor, which is crystalline, as indicated by sharp peaks at $2\theta \approx 9°$, 10°, etc. At 300° and 500°C, the XRD patterns exhibit broad maxima, characteristic of amorphous material. At 700°C, crystallization of β-$BaO{\cdot}SiO_2$ takes place, as evidenced by a peak at $2\theta \approx 26°$ (JCPDS File 26-1402). At 900° and 1000°C, other peaks, at $2\theta \approx 26.5°$, 28°, etc., develop and sharpen in intensity, due to crystal growth. These results are in agreement with the DRIFTS and SEM studies discussed below.

(C) DRIFTS: The DRIFT spectra for the Ba precursor, before and after heating to selected temperatures, are displayed in Fig. 5. The spectra resemble those observed for the pentacoordinated group I complexes and their decomposition products. Thus, the starting material (170°C) shows ν(O–H) bands centered at 3300 cm^{-1}, due to the EG solvate molecules, and ν(C–H) bands at 2800–3000 cm^{-1}. The bands in the 1050–1140 cm^{-1} region correspond to a combination of ν(Si–O) and ν(C–O) vibrations. The 300°C material exhibits two relatively intense absorption bands at 1430 and 1570 cm^{-1}. The 1430 cm^{-1} band is ascribed to the formation of amorphous or nanocrystalline (since it is not seen by XRD) $BaCO_3$. The same band is observed in an authentic sample of pure $BaCO_3$ (see Fig. 6) and also confirmed by the literature.[9] The peak at 1570 cm^{-1} may result from barium bicarbonate by analogy with the alkali carbonates.[6,9] These relatively sharp bands reflect the considerable quantities (50 wt%) of $BaCO_3$ that are present in the 300°C material.

At 500° and 700°C, the 1570 cm^{-1} band becomes smaller and finally disappears by 900°C. The band at 1430 cm^{-1} continues to be prominent in the 700°C spectrum, but finally disappears at

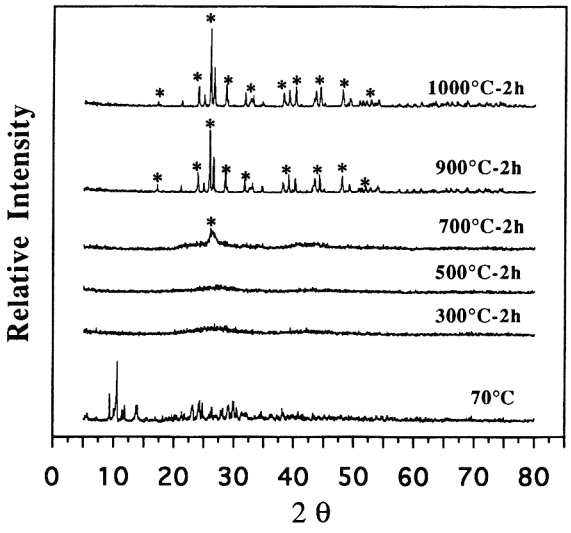

Fig. 4. XRDs of $BaSi(OCH_2CH_2O)_3$ pyrolyzed to selected temperatures, 2-h hold; * indicates β-$BaO{\cdot}SiO_2$, JCPDS File 26-1402.

900°C with the decomposition of $BaCO_3$ (T_d = 980°C). The DTA and TGA studies, presented above, corroborate these results/observations. The fact that no $BaCO_3$ bands are seen in the 900°C spectrum, despite the fact that it is stable to 980°C, reflects the fact that the pyrolysis temperature is near the decomposition temperature and the bulk pyrolyses were run with 2-h dwell times at selected temperatures. In addition, the decomposition is driven by the formation of $BaO{\cdot}SiO_2$.

In the DRIFT spectra, sharp peaks appear below <1100 cm^{-1} at 900° and 1000°C, which match the fingerprint region of β-$BaO{\cdot}SiO_2$. We assign the band at 1020 cm^{-1} to an asymmetric ν(Si–O–Si) vibration and the band at 910 cm^{-1} to ν(Si–O) of nonbridging oxygens (Si–O^-Ba^{2+}).[10–13] The peak at 750 cm^{-1}

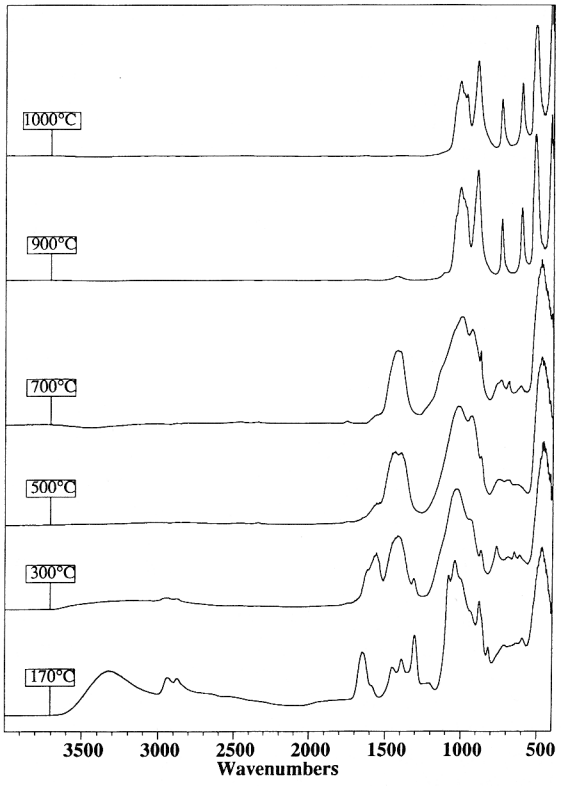

Fig. 5. DRIFTS of $BaSi(OCH_2CH_2O)_3$ pyrolyzed to selected temperatures, 2-h hold.

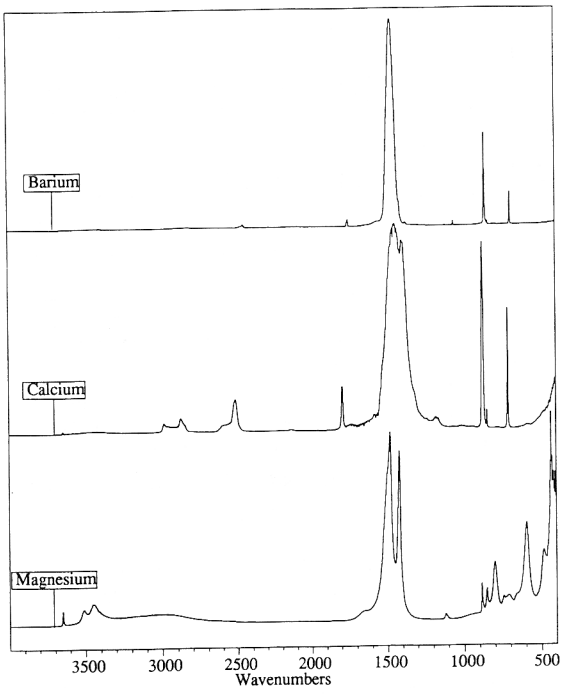

Fig. 6. DRIFTS of group II carbonates.

likely arises because of contributions from ν(Si–O–Si) symmetric vibrations and the peak at 530 cm^{-1} may be due to a δ(Si–O–Si) bending motion.

(D) Scanning Electron Microscopy: The SEM micrographs seen in Figs. 7(a–c) provide a clear picture of the morphological changes (crystallization) that occur in the three materials. The 500°C micrograph (Fig. 7(a)) shows vague features typical of an amorphous material. Likewise, the 700°C micrograph (Fig. 7(b)) suggests an amorphous material corroborating the XRD, FTIR, and DTA data. In contrast, the micrograph of the 1000°C material (Fig. 7(c)) reveals significant crystallization and grain growth. Indeed, the lack of porosity in the region shown suggests extensive sintering. Other regions show similar grain growth with some pores remaining. The extent of grain growth and the lack of porosity may indicate the formation of a liquid phase during $BaCO_3$ decomposition and coincident $BaO{\cdot}SiO_2$ crystallization. At this time, we have no support for this conjecture. These results are in contrast to the SEM studies of the crystallization of the other two silicates which suggest the formation of very fine grain structures on crystallization, as discussed below.

(2) $CaSi(OCH_2CH_2O)_3$

(A) Thermal Analysis: TGA of 70°C, vacuum-dried powder $CaSi(OCH_2CH_2O)_3{\cdot}3HOCH_2CH_2OH$ (see Experimental Section) gave a ceramic yield of 27.0%. Assuming the end product to be $CaO{\cdot}SiO_2$ at 1000°C, the number of EG molecules of recrystallization per silicon center was calculated to be 3.00, similar to the Ba analogue. This was confirmed by chemical analysis (see Table I), which shows an experimental value for C of 32.53 wt%, against a calculated value of 33.15. Likewise, the experimental value for H is 6.70 wt% as opposed to a calculated value of 6.91. Both results are within the error limits of the analytical technique.

The crystalline nature of this solvate complex is evidenced by its XRD powder pattern (see below). The EG solvate molecules are removed on heating at 170°C (4–5 h) under vacuum and the precursor powder is no longer crystalline. The resulting precursor conforms to the formula $CaSi(OCH_2CH_2O)_3$, as confirmed by TGA (see below). The TGA (Fig. 1) found ceramic yield for the 170°C material is 45.5% versus 46.8% calculated (Table II). The small mass difference is again likely due to residual EG solvate molecules. The initial mass loss in the range of 170–360°C is due to oxidative decomposition of the glycolate ligands. The 5% mass loss at 850–885°C is due to decomposition of $CaCO_3$ (T_d = 898°C). Similar to the Ba analogue, assuming the entire mass loss to be due to CO_2 evolution, the mass of $CaCO_3$ present in the sample prior to decomposition is calculated to be 22.5%, which is considerably less than seen in the Ba material. The apparent stoichiometric distribution of compounds below ≈850°C is $2.4CaO{:}CaCO_3{:}3.4SiO_2$. Thus, $CaCO_3$ accounts for only 33 mol% of all of the calcium species present rather than ≈50%, as in the case of barium.

The DTA (Fig. 2) exhibits a single exotherm at 266°C as a result of oxidative decomposition of the glycolatosilicate to form amorphous $CaO{\cdot}SiO_2$ (see XRD below). This is some 60–100°C lower than any of the group I silicates. The large exotherm at 910°C is likely due to crystallization of pseudowollastonite, α-$CaO{\cdot}SiO_2$, as corroborated by XRD studies which follow. Given that the TGA results indicate the loss of CO_2 in the same temperature region, crystallization appears to occur coincident with decomposition of $CaCO_3$; consequently, no endotherm is observed for the decomposition process.

(B) XRD: The XRD patterns displayed in Fig. 8 show the phase development upon pyrolysis at selected temperatures. The material dried at 70°C is crystalline, as indicated by the well-resolved powder pattern. Samples decomposed at 300°, 500°, and 700°C do not exhibit any crystallinity whatsoever. Their XRD powder patterns are almost featureless. On heating to 900° and 1000°C, crystallization is indicated by sharp peaks at $2\theta \approx 27.5°, 32°, 45.5°$. These peaks correspond to pseudowollastonite, α-$CaO{\cdot}SiO_2$ phase (JCPDS File 31-300).

(C) DRIFTS: The DRIFT spectra are displayed in Fig. 9. Like the Ba complex, the starting material exhibits ν(O–H) bands centered at 3300 cm^{-1} due to EG solvate molecules and ν(C–H) bands at 2800–3000 cm^{-1}. These bands are not observed in the pyrolyzed product spectra at 300°, 500°, and 700°C, which display broad, diffuse absorption bands, characteristic of amorphous, inorganic materials. As with the Ba silicate, prominent absorptions at 1430 and 1580 cm^{-1} in the 300°C spectrum are consistent with formation of $CaCO_3$ and $Ca(HCO_3)_2$. The presence of $CaCO_3$ was again corroborated by taking a spectrum of pure $CaCO_3$ (Fig. 6) and by the literature.[9] Again, the absence of a $CaCO_3$ powder pattern in the XRD suggests that any $CaCO_3$ present is either amorphous or nanocrystalline. The relatively sharp bands are due to the large amounts of $CaCO_3$ (22.5%) as determined by the TGA mass loss. Note that the carbonate bands are not as strong as seen for $BaCO_3$, because of the lesser amounts of $CaCO_3$ (22% vs 50%). The band at 1580 cm^{-1} results from calcium bicarbonate by analogy with the alkali carbonates.[6,9] These bands diminish at 500° and 700°C, and finally disappear at 900°C, as expected given that T_d for $CaCO_3$ is 898°C. DTA and TGA studies corroborate the DRIFT data.

Samples pyrolyzed to 900° and 1000°C exhibit a series of sharp absorption bands at <1100 cm^{-1} that match the fingerprint region of pseudowollastonite. Again, the bands at 1000 and 1100 cm^{-1} are due to an asymmetric ν(Si–O–Si) absorption and a ν(Si–O) band appears at 945 cm^{-1}, indicating the presence of nonbridging oxygens ($Si{-}O^{-}Ca^{2+}$).[10–13] The peak at 735 cm^{-1} can be attributed to contributions from ν(Si–O–Si) symmetric vibrations. The peak at 580 cm^{-1} is similar to that seen in the barium compound and is due to δ(Si–O–Si) bending motions.

(D) SEM: The SEM micrograph of Ca precursor pyrolyzed to 1000°C (Fig. 10) contrasts considerably with those for pyrolyzed Ba precursor (Figs. 7(a–c)), where crystallization is quite clear. The appearance of very fine particle sizes (Fig. 10) can be rationalized as retention of the good atomic mixing in the precursor as it is pyrolytically transformed into an amorphous, intermediate phase and then heated to successively higher temperatures. The sharp crystallization exotherm at 910°C could be construed as supporting the high degree of mixing, if one assumes that poor atomic mixing will require energy for diffusion of the component atoms and thereby draw from the energy

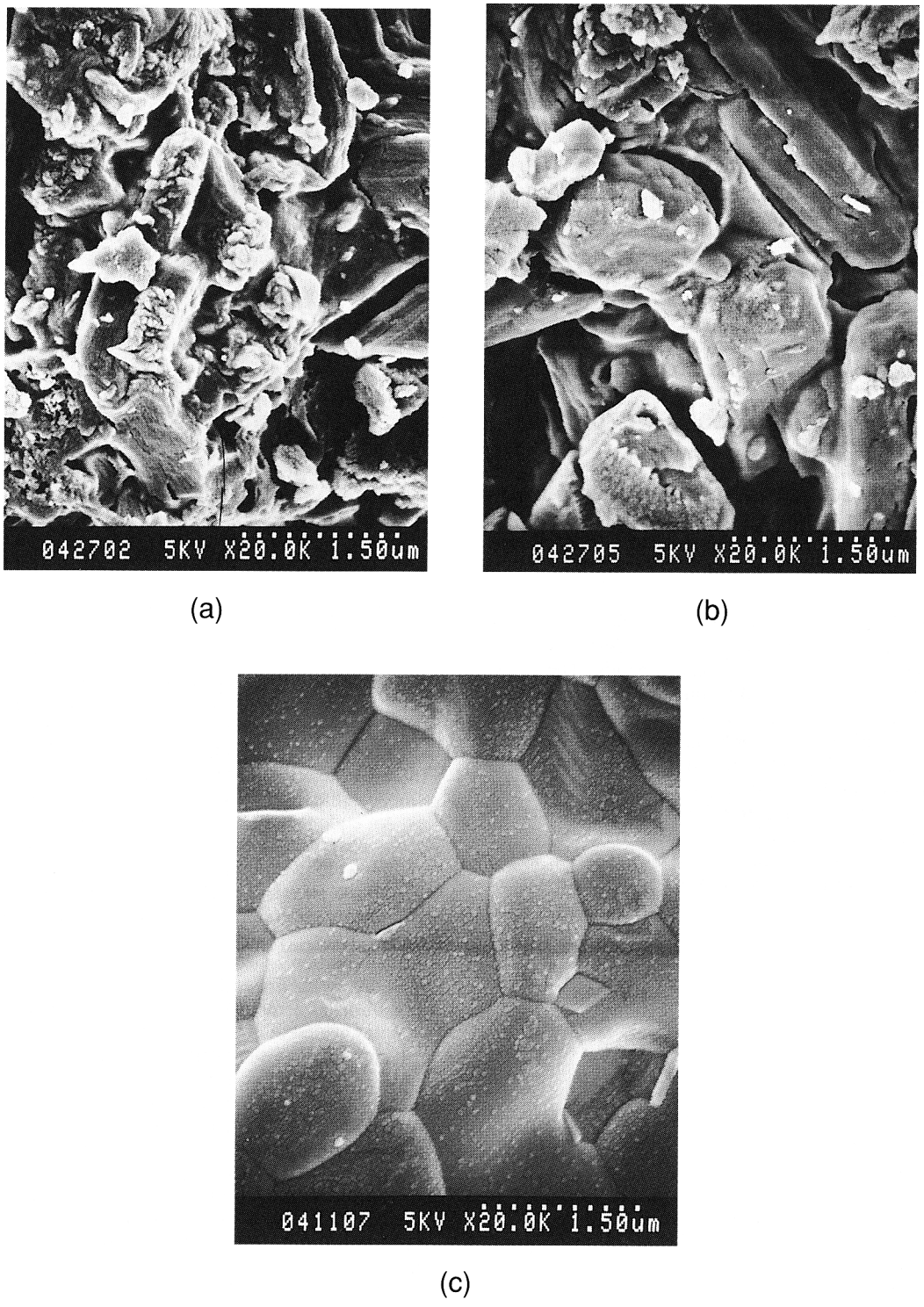

Fig. 7. SEMs of $BaSi(OCH_2CH_2O)_3$ pyrolyzed to (a) 500°, (b) 700°, (c) 1000°C, 2-h hold.

generated during crystallization. This contrasts with the argument used above to explain the lack of a strong exotherm in the Ba studies. An alternate explanation is that decomposition and crystallization are not accompanied by the formation of a liquid phase that aids in sintering.

(3) $MgSi(OCH_2CH_2O)_3$

(A) Thermal Analyses: Following the same pattern of characterization as for the Ba and Ca products, the TGA ceramic yield for the 70°C material was found to be 27.1%, which suggests the presence of several EG solvate molecules. Again assuming pure $MgO{\cdot}SiO_2$ end product and pure starting material, the number of EG molecules of recrystallization per silicon center was calculated to be 2.25. This was confirmed by chemical analysis (Table I), which provides experimental values for C and H of 33.98 and 7.19 wt%, respectively, for $MgSi(OCH_2CH_2O)_3{\cdot}2.25HOCH_2CH_2OH$ vs calculated values of 33.89 and 6.85, respectively. As above, these values are within experimental error. The fact that the analyses for all three compounds are all very close points to the high purity with which these compounds can be made in just one step.

The XRD powder pattern (see below) shows that the 70°C-dried solvated complex is crystalline. Like the other group II glycolatosilicates, heating at 170°C (4–5 h) under vacuum removes the EG solvate molecules resulting in an amorphous, essentially pure, solvent-free, $MgSi(OCH_2CH_2O)_3$ precursor, as confirmed by TGA. The TGA profile (Fig. 1)

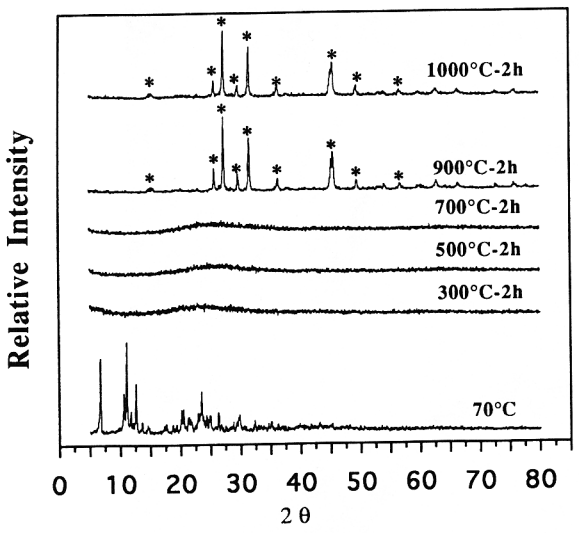

Fig. 8. XRDs of $CaSi(OCH_2CH_2O)_3$ pyrolyzed to selected temperatures, 2-h hold; * indicates pseudowollastonite, $CaO{\cdot}SiO_2$, JCPDS File 31-300.

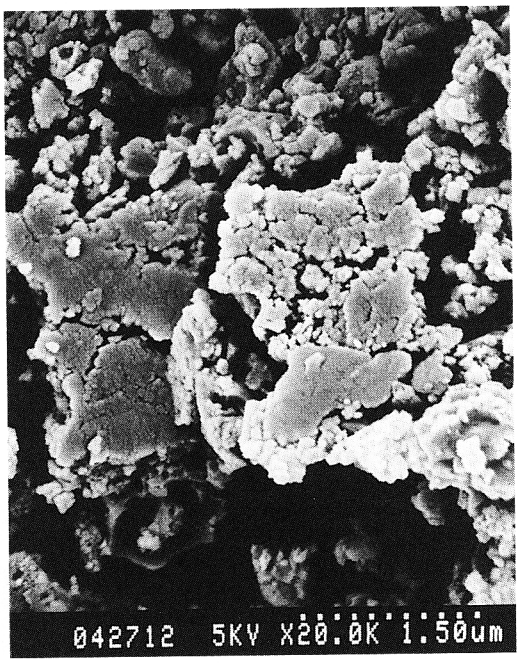

Fig. 10. SEM of $CaSi(OCH_2CH_2O)_3$ pyrolyzed to 1000°C, 2-h hold.

shows a ceramic yield of 42.5% against the calculated value of 43.2% (Table II). The initial weight loss at 200–340°C is due to oxidative decomposition of the glycolate ligands. The 3.6% mass loss observed just above 900°C must result from decomposition of magnesium carbonate (T_d = 900°C), based on our observations concerning the Ca and Ba derivatives. By back calculating, the mass of $MgCO_3$ is found to be 15 wt%. This is further confirmed by DRIFTS studies, as discussed below. The apparent composition of the material just below 900°C can be given as $4.1MgO{:}MgCO_3{:}5.1SiO_2$.

The DTA (Fig. 2) shows exotherms at 190° and 310°C which result from oxidation of the glycolato ligands, as corroborated by the weight loss in TGA. As mentioned for barium glycolatosilicate, the exotherm at 190°C may also result from oxidation of the residual EG solvate molecules of recrystallization. The 310°C exotherm results from oxidation of the glycolate ligands. The broad exotherm at 970°C coincides with crystallization of clinoenstatite, $MgO{\cdot}SiO_2$, as confirmed by the following studies. An endotherm corresponding to decomposition of $MgCO_3$ is not observed, most likely because of the relatively small amounts (15 wt%) present. The relatively broad exotherm appears to correlate with the slow weight loss, in the same temperature range, that corresponds to $MgCO_3$ decomposition.

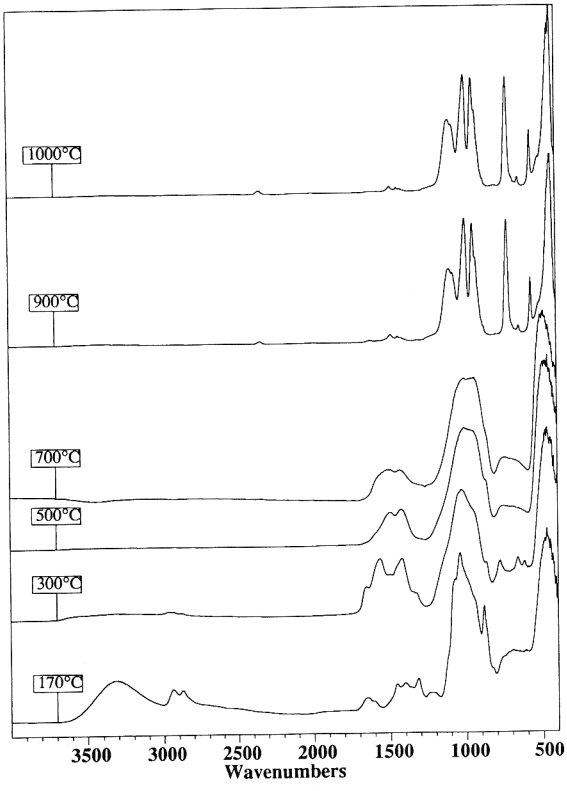

Fig. 9. DRIFTS of $CaSi(OCH_2CH_2O)_3$ pyrolyzed to selected temperatures, 2-h hold.

(B) XRD: Figure 11 XRD powder patterns record the phase evolution as samples are pyrolyzed to selected temperatures. As with Ba and Ca complexes, the 70°C complex is crystalline, as demonstrated by the well-defined powder pattern. Samples heated to 300°, 500°, and 700°C are X-ray amorphous, also supported by the DRIFTS studies. On heating to 900° and 1000°C, samples finally crystallize to the monoclinic, clinoenstatite phase of $MgO{\cdot}SiO_2$ (JCPDS File 35-610), as evidenced by peaks at $2\theta \approx 27.5°, 30.0°, 35.5°$. The fact that crystallization in the bulk samples is observed at 900°C, rather than at 970°C as seen in the DTA, occurs because the XRD samples were held at the selected temperature for 2 h, aiding in diffusion, which in turn results in crystallization at a lower temperature. The material appears to be phase pure, on comparison with the JCPDS file.

(C) DRIFTS: DRIFT spectra are displayed in Fig. 12. As typical with these materials, the starting material (170°C) shows a ν(O–H) band centered at 3300 cm^{-1}, due to free EG and ν(C–H) bands at 2800–3000 cm^{-1}. The spectra at 300°, 500°, and 700°C are similar to those observed for the Ba and Ca materials. They exhibit carbonate bands at 1430 and 1620 cm^{-1}. The presence of $MgCO_3$ is confirmed by comparison with an authentic sample (see Fig. 6) and by the literature.[9] The band at 1620 cm^{-1} may also arise because of the presence of magnesium bicarbonate, by analogy with the Ba and Ca carbonates as identified above.[6,9] These bands are not as sharp as seen in the $BaO{\cdot}SiO_2$ and $CaO{\cdot}SiO_2$ spectra, because only small quantities of metal carbonate (15%) are present as discussed above. The band at 1430 cm^{-1} disappears at 500°C, while the band at 1620 cm^{-1} becomes smaller and finally disappears at 900°C (T_d = 900°C), corroborated by mass loss in the TGA, due to decomposition of $MgCO_3$. Because bicarbonates decompose at temperatures much below their respective carbonates, it is

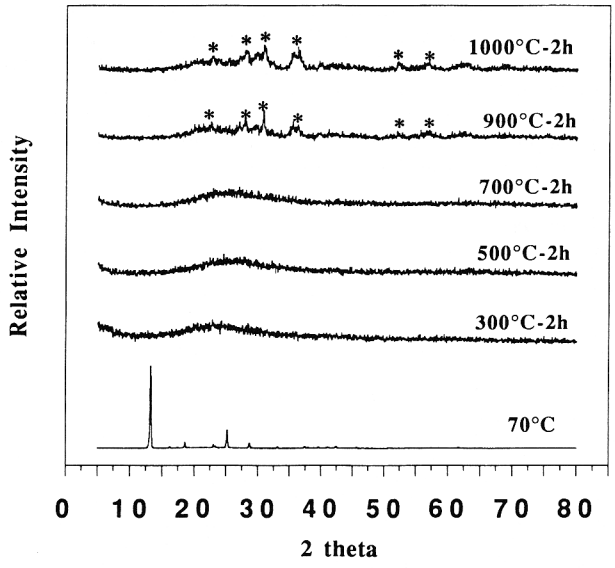

Fig. 11. XRDs of $MgSi(OCH_2CH_2O)_3$ pyrolyzed to selected temperatures, 2-h hold; * indicates clinoenstatite, $MgO{\cdot}SiO_2$, JCPDS File 35-610.

difficult to say whether the band at 1620 cm^{-1} is due to the bicarbonate (by analogy) or due only to the carbonate; see the spectrum of $MgCO_3$ (Fig. 6).

As with the Ba and Ca compounds, Mg samples heated to 900° and 1000°C exhibit a series of sharp absorption bands at <1100 cm^{-1} that match the fingerprint region of clinoenstatite. The bands at 1080 and 960 cm^{-1} are ascribed to an asymmetric ν(Si–O–Si) absorption and the ν(Si–O) of $Si–O^-Mg^{2+}$ species, respectively.[10–13] The peaks at 760 and 790 cm^{-1} are assumed to result from ν(Si–O–Si) symmetric vibrations. The DRIFT spectra correlate well with the XRD patterns.

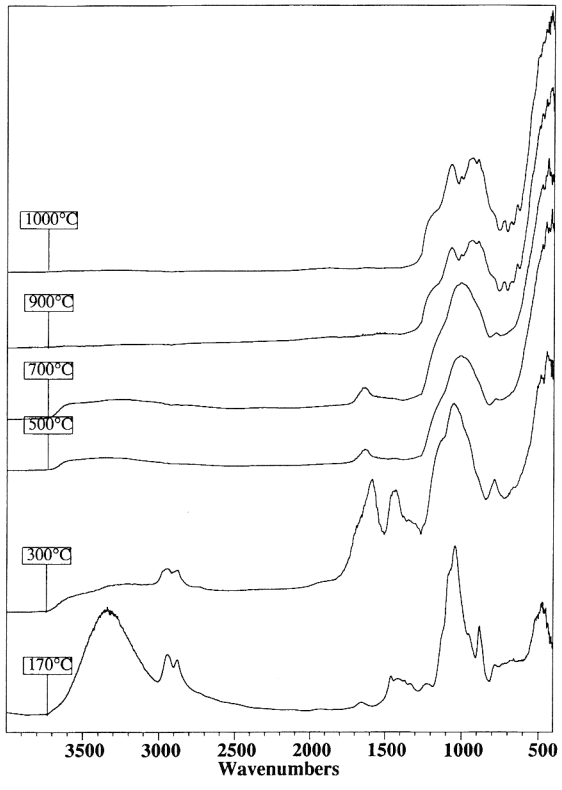

Fig. 12. DRIFTS of $MgSi(OCH_2CH_2O)_3$ pyrolyzed to selected temperatures, 2-h hold.

(D) SEM: The micrograph seen in Fig. 13 is similar to Fig. 10, showing only very fine grains of $MgO{\cdot}SiO_2$. The same arguments as made above for the formation of the microstructure observed for 1000°C $CaO{\cdot}SiO_2$ can be made for crystallization of $MgO{\cdot}SiO_2$. Good atomic mixing and/or the absence of a liquid phase that aids sintering during carbonate decomposition are both rationales for why a fine-grained material forms.

To summarize, the alkaline-earth glycolatosilicates exhibit very similar behavior on pyrolysis. All the synthesized precursors (vacuum dried at 70°C) are crystalline, EG solvates, as shown by sharp peaks in XRD, chemical, and TG analyses. The EG solvent molecule engendered crystallinity is lost once the complexes are heated to 170°C *in vacuo*. The TGAs of the 170°C products suggest that they conform to the $MSi(OCH_2CH_2O)_3$ formula, based on found ceramic yield. All the precursors show mass losses between 170° and 400°C due to oxidative decomposition of the glycolate ligands. These events are corroborated by DTA, which shows exotherms in this temperature range. Lower-temperature exotherms in barium (270°C) and magnesium (190°C) glycolatosilicate DTAs most likely result from oxidation of residual EG solvate molecules, even though the precursors were heated at 170°C for 4–5 h prior to pyrolysis.

On pyrolysis above 300°C, all of the resulting products are amorphous and contain significant amounts of group II metal carbonates (by DRIFTS, TGA, and DTA). The carbonate band positions and thermal behavior of the carbonates were established by comparison with standard published spectra and also by characterizing authentic samples of these metal carbonates. Similar carbonate bands were also seen in group I alkali silicates due to the formation of alkali carbonates which further helped in identification. Because samples were pyrolyzed in dry, synthetic air free of CO_2 or H_2O, the source of CO_2 must result from capture of CO_2 evolved during pyrolysis (removal of EG ligands) of the EG groups. The calculated weight percent of metal carbonates is maximum for Ba (50%) and minimum for Mg (15%) with Ca (22%) in between. This is expected as Ba has the highest affinity for CO_2 and Mg the least, based on their positions in the periodic table. The carbonate stabilities for group I and II metals increase on descending a particular column of the periodic chart, as we have previously noted.[6]

The carbonates dominate the crystallization process in the Ba compound, have no effect in the Ca compound as evidenced by the very sharp exotherm in the DTA, and seem to also play a role in broadening the crystallization temperature range for

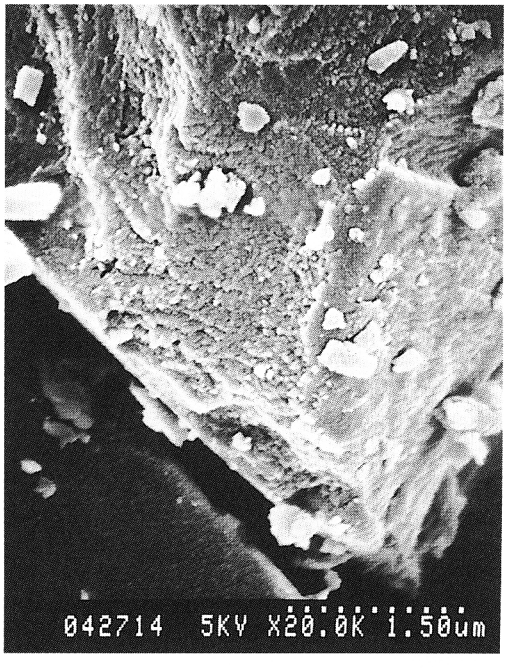

Fig. 13. SEM of $MgSi(OCH_2CH_2O)_3$ pyrolyzed to 1000°C, 2-h hold.

the Mg compound. The large percentage of barium carbonate explains the minor decomposition endotherms and crystallization exotherms in the barium glycolatosilicate DTA. The results suggest that segregation occurs during the initial decomposition process, perhaps driven by formation of $BaCO_3$. At higher temperatures, any energy produced by exothermic crystallization is spent in promoting further decomposition of $BaCO_3$ or diffusion of segregated species that eventually results in the formation of $BaO{\cdot}SiO_2$.

In contrast, $CaO{\cdot}SiO_2$ exhibits a sharp exotherm at 910°C due to crystallization with no evidence of an underlying endotherm for $CaCO_3$ which is expected to occur at the same temperature. The magnesium silicate shows a broad exotherm at 970°C due to crystallization. We can suggest that a small endotherm expected for $MgCO_3$ decomposition at 900°C (mass loss seen in TGA) is probably hidden below the exotherm. The higher-temperature XRD patterns for the calcium and barium silicate compounds show sharp, well-defined powder patterns, whereas the magnesium silicate shows diffuse intensities, despite the exotherm seen in the DTA.

IV. Conclusions

The hexacoordinate glycolatosilicates behave similarly to the pentacoordinate species. The decomposition and crystallization patterns are similar. The important point to note is that all hexacoordinate silicates crystallize by 900°C into phase-pure monosilicates unlike pentacoordinate glycolates which show some phase segregation (Li, K).[6] The TGA found ceramic yields in all of the hexacoordinate precursors were typically low by 1–2% due to residual amounts of EG molecules of recrystallization. These results indicate that we were able to synthesize stoichiometric starting materials which on pyrolysis give phase-pure ceramic products.

All of the alkaline-earth glycolatosilicates oxidatively decompose to an amorphous phase at ≈300°C, as determined by both the DRIFTS spectra and XRD patterns. Even though the bulk decomposition studies were run in flowing, dry air, a great part of the CO_2 produced during ligand oxidation is captured by the intermediate pyrolysis products, leading to the formation of metal carbonates (15–50%). Though care was taken not to expose the DRIFTS samples to the air, some CO_2 may have been captured during the transfer from the glove box to IR chamber. All of the intermediates recovered following pyrolysis to 700°C remain amorphous and exhibit some evidence for the presence of carbonate species, as identified by DRIFTS. At 900°C, the intermediates crystallize into phase-pure $MO{\cdot}SiO_2$.

These studies indicate that it is possible to transform $MSi(OCH_2CH_2O)_3$ (where M = Ba, Ca, or Mg) into phase-pure silicates. Exchange of EG with longer-chain diols leads to processable polymers that may give access to thin films, fibers, and coatings. As we will show in future papers, it is possible to use the group II glycolatosilicates as components in the preparation of rheologically useful aluminosilicates.[14]

References

[1](a) R. M. Laine, K. Y. Blohowiak, T. R. Robinson, M. L. Hoppe, P. Nardi, J. Kampf, and J. Uhm, "Synthesis of Novel, Pentacoordinate Silicon Complexes from SiO_2," *Nature (London)*, **353**, 642–44 (1991). (b) K. Y. Blohowiak, M. L. Hoppe, K. W. Chew, P. Kansal, B. L. Mueller, C. L. S. Scotto, T. Hinklin, F. Babonneau, J. Kampf, and R. M. Laine, "SiO_2 as a Starting Material for the Synthesis of Pentacoordinate Silicon Complexes. I," *Chem. Mater.*, **6**, 2177–92 (1994).

[2]K. A. Youngdahl, P. Nardi, T. R. Robinson, and R. M. Laine, "The Synthesis of Novel Penta-Alkoxy and Penta-aryloxy Silicates from Silica"; pp. 99–114 in NATO Advanced Study Institutes Series, Series E: Applied Sciences, Vol. 206, *Inorganic and Organometallic Polymers with Special Properties*. Edited by R. M. Laine. Kluwer Publishers, Dordrecht, Netherlands, 1991.

[3]C. R. Bickmore, M. L. Hoppe, R. M. Laine, K. A. Youngdahl, P. Nardi, T. R. Robinson, and J. Uhm, "Chemicals, Polymers and Ceramics from the Beach (Silica)"; pp. 663–71 in the Proceedings of the 5th International Conference on Ultrastructure Processing. Edited by L. L. Hench and J. K. West. Wiley, New York, 1992.

[4]C. R. Bickmore, M. L. Hoppe, and R. M. Laine, "Processable Oligomeric and Polymeric Precursors to Silicates Prepared Directly from SiO_2, Ethylene Glycol and Base"; pp. 107–14 in Materials Research Society Symposia Proceedings, Vol. 249, *Synthesis and Processing of Ceramics: Scientific Issues*. Edited by W. E. Rhine, T. M. Shaw, R. J. Gottschall, and Y. Chen. Materials Research Society, Pittsburgh, PA, 1991.

[5]M. L. Hoppe, R. M. Laine, J. Kampf, M. S. Gordon, and L. W. Burggraf, "Barium Tris(glycolato)silicate, a Hexacoordinate Alkoxy Silane Synthesized from SiO_2, *Angew. Chem. Int. Ed. Engl.*, **32**, 287–89 (1993).

[6]P. Kansal and R. M. Laine, "Pentacoordinate Silicon Complexes as Precursors to Silicate Glasses and Ceramics," *J. Am. Ceram. Soc.*, **77**, 875–82 (1994).

[7]Z.-F. Zhang, M. L. Hoppe, J. A. Rahn, S.-M. Koo, and R. M. Laine, "Low Temperature Routes to Cordierite-like Ceramics Using Chemical Processing"; pp. 81–86 in Materials Research Society Symposia Proceedings, Vol. 249, *Synthesis and Processing of Ceramics: Scientific Issues*. Edited by W. E. Rhine, T. M. Shaw, R. J. Gottschall, and Y. Chen. Materials Research Society, Pittsburgh, PA, 1991.

[8]Q. Zheng and D. D. L. Chung, "Microporous Calcium Silicate Thermal Insulator," *Mater. Sci. Technol.*, **6**, 666–69 (1990).

[9]Sadtler High Resolution Spectra of Inorganics and Related Compounds, Sadtler Research Laboratories, Philadelphia, PA, 1965.

[10]T. Uchino, T. Sakka, K. Hotta, and M. Iwasaki, "Attenuated Total Reflectance Fourier-Transform Infrared Spectra of a Hydrated Sodium Silicate Glass," *J. Am. Ceram. Soc.*, **72**, 2173–75 (1989).

[11]F. Domine and B. Piriou, "Study of Sodium Silicate Melt and Glass by Infrared Reflectance Spectroscopy," *J. Non-Cryst. Solids*, **55**, 125–30 (1983).

[12]T. Uchino, T. Sakka, and M. Iwasaki, "Interpretation of Hydrated States of Sodium Silicate Glasses by Infrared and Raman Analysis," *J. Am. Ceram. Soc.*, **74**, 306–13 (1991).

[13]S. A. Brawer and W. B. White, "Raman Spectroscopic Investigations of the Structure of Silicate Glasses. I. The Binary Alkali Silicates," *J. Chem. Phys.*, **63**, 2421–32 (1975).

[14]P. Kansal and R. M. Laine; unpublished results. □